ECI Symposium Series, Volume RP5: Proceedings of 7th International Conference on Heat Exchanger Fouling and Cleaning - Challenges and Opportunities, Editors Hans Müller-Steinhagen, M. Reza Malayeri, and A. Paul Watkinson, Engineering Conferences International, Tomar, Portugal, July 1 - 6, 2007

A LAGRANGIAN PARTICLE CFD POST-PROCESSOR DEDICATED TO PARTICLE ADHESION/DEPOSITION

M. Losurdo[1], C. Bertrand[2] and H.Spliethoff[3]
[1] TU Delft, Leeghwaterstraat 44, 2628 CA Delft, The Netherlands; m.losurdo@tudelft.nl
[2] ECN, P.O. Box 1, 1755 ZG Petten, The Netherlands; bertrand@ecn.nl
[3] TU Munich, Boltzmannstr. 15, 85748 Garching, Germany; spliethoff@tum.de

ABSTRACT

In the past few years the use of biomass in power plants has grown dramatically. As a result of this action fouling and slagging in co-firing biomass facilities have turned out to play a critical role in the efficiency of such facilities. Efficient and effective methods are therefore needed to control fouling to an acceptable level and to prevent economic losses due to reduced furnace thermal efficiency, increased maintenance or even unscheduled outages. Numerical prediction of the impact of deposit properties has proved itself to be a successful strategy to both evaluate changes in the facility performance and to investigate possible solutions to minimize fouling as well. TU Delft and ECN started a project to monitor and control fouling in furnaces co-firing biomass with coal by means of numerical simulations and experiments. Numerical investigations are based on the development of a novel in-house code to track solid particles post-processing gas phase CFD data. These have been calculated using commercial codes such as FLUENT, CINAR and CFX. The Lagrangian Particle Post-Processor code (P^3) strategy and numerical results are presented here. Numerical simulation compare fairly well to the available experimental data for glass particles.

INTRODUCTION

During the last decade, prediction of particle deposition in both cold (like ventilation pipelines and air conditioning conducts where dust deposits) and hot facilities (like coal and biomass burners where ash particles deposit on walls and heat exchangers) has become a very important issue. In the present work we focused our attention to power generation facilities burning coal together with biomasses. Numerical prediction of ash formation and deposition, fouling and slagging, that occur when co-firing biomass, can be considered as an important support to evaluate the impact of deposition overall boiler performance (Baxter et al. 1992, Srinivasachar et al. 1990). Given the mathematical description of a such complex phenomena, computer modelling may represent a more appropriate tool than empirical indices based on coal ash compositions to describe deposition process . The aim of this work is to provide a post-processor tool that can elaborate and integrate CFD and ash cross correlation data in order to predict flying ash deposit behavior, deposit growth and heat transfer performance. This aim can be achieved by developing a CFD-independent particle tracking code that follows particles within the given computational domain and numerically predicts extent properties and impact of deposit. This work deals with the transportation and deposition of glass particles on one steam pipe thermally monitored. The P^3 particle diffusion model has been validated comparing numerical results with Snyder and Lumley results. The particle deposition model is validated using ECN glass and biomass ash experimental results. The P^3 code predicts the location and the characteristics of fouling for a given combination of fuel (hence ash composition) and operating conditions, and can be used for process optimization. In addition, a real-time deposit evaluation enables researchers to predict deposition while particles are being tracked; wall surface viscosity, the composition, the thermal resistance and the deposit thickness are modified during the computation to the deposited particle properties. In this way it is possible to study deposit on clean and not-clean surfaces during the same computation. Therefore, it is possible to collect time dependent numerical results to be compared to the on-line monitored ones if available. Depending on the facility, tube diameters, the investigated time frame and particle properties, deposit thickness may influence the fluid dynamics of the system. At the present time the P^3 code is capable of exporting deposit results to FLUENT and to restart the CFD computation (see Fig. 1a and 1b) over the modified geometry.

Experiments have identified several processes including chemical and physical phenomena which cause particles to deposit. These processes are for example referred to inertia impaction, (turbulent) diffusion, thermophoretic attraction, vapor condensation and heterogeneous reaction between ash particles and deposition surfaces. Thermophoresis, condensation and inertia impaction are addressed as the most relevant processes that contribute to the deposit growth (Baxter and De Sollar 1993, Huang et al. 1996, He and Ahmadi 1998). Since these phenomena can all occur along the furnace, they have to be considered and evaluated together with specific and dedicated computational tools.

The main motivations to develop an in-house particle tracking code as foursome are:

1. to increase researchers numerical investigation potential without compromise previous commercial agreements with CFD companies

2. to increase partnerships and cooperation between institutes by means of an unstructured particle tracker code capable of reconstruct any P1 finite element mesh.
3. to overcome some of the several limitation of current particle modeling commercial CFD codes.
4. to investigate the deposition/particle stickiness phenomena using a novel computational and modeling strategy which could not be implemented in a straight forward manner into any commercial CFD code.

THE P^3 NUMERICAL STRATEGY

The P^3 code is a particle tracking post-processor which is capable of reading and reconstructing hybrid unstructured CFD meshes (P1 finite elements) based on topological node information (inlet, outlet and wall). The detection of the cell, in which the particle is located, consists in a two step particle bounding box algorithm whose CPU requirements are quasi-independent of the mesh size (computational nodes). One of the main issues in developing and performing a Lagrangian particle tracking is represented by the computational time required for the particle cell detection. The presented two step tracking particle algorithm has been developed to comply with computational efficiency and accuracy (particle lost during the computation). The first step consists in highlighting the particle surrounding volume (the smallest region that contains the particle) and the group of cells which are included in this volume. In the second step, the cell which contains the particle, is found by means computing the distance from the cell boundary faces: distances of a given cell are all positive only if that cell contains the particle. Instead of performing such a calculation on every cell of the computational domain, the loop is set up only on those cells which are enclosed in the particle surrounding volume. The Trilinear Isoparametrical algorithm is used both to calculate the distances from the cell faces and to interpolate nodes variables at the particle location. The CPU requirements for this algorithm can be considered essentially independent from the volume and the size of the computational domain as it loops only on the particle surrounding volume (see Fig. 2). Usually, the computation is limited to a maximum of 5-7 cells if a tetrahedral mesh is used while, for regular hexahedral meshes, the correct cell is usually detected during the first step.

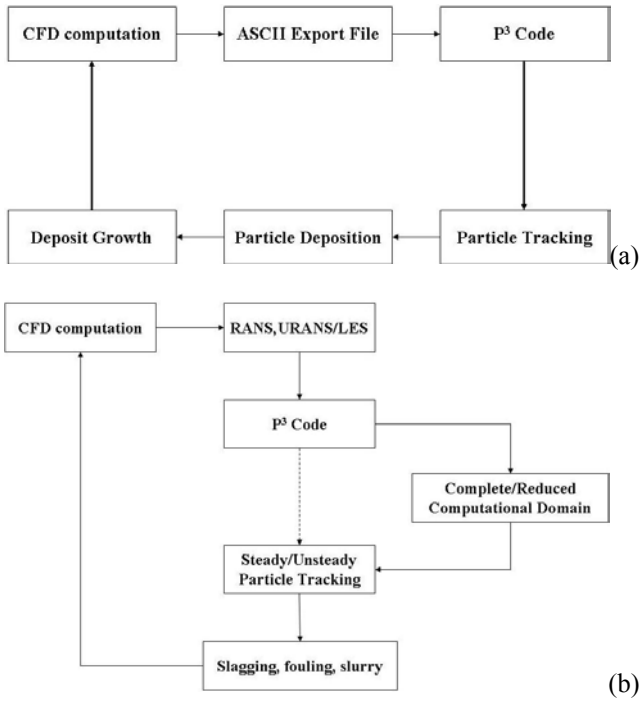

Fig. 1 (a) and (b) Schemes of the main P^3 algorithms: general overview.

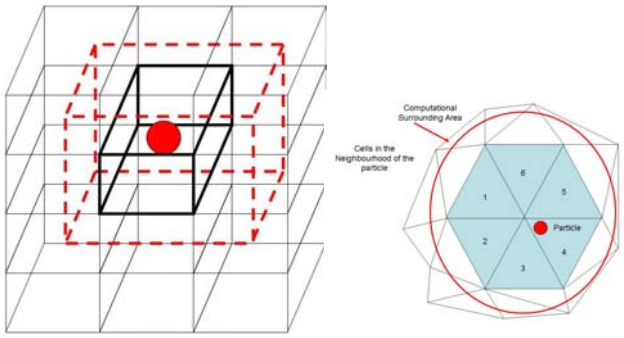

Fig. 2 Bounding Box Approach in particle detection. a) hexahedral mesh, b) tetrahedral mesh

Several features of the P^3 code can be highlighted:

1. Combined use of steady/unsteady particle tracking in the complete and/or reduced computational domain.
2. Multi-Gaussian distribution functions to characterize the properties of groups and clusters of particles.
3. Trilinear Isoparametric Interpolation (TII) 1+n iteration, where n represents the additional number of iterations required to achieved the desired accuracy in the calculation. n is usually smaller than 3 since the first iteration is performed using a rough estimation of the particle position normalized by the cell dimension. This algorithm has been developed for the second step of the particle cell detection since it converts a distorted cell into a regular plain cell

(pyramids, wedges and hexahedra). This algorithm allows to move mesh nodes according to the deposit without decreasing particle detection accuracy.
4. Steady/unsteady CFD calculations (RANS κ-ε model, URANS and LES) are successfully used as input for the P^3 to better evaluate the influence of turbulence (unsteady flow field) in the particle transport and deposition process
5. Real Time Deposit Evaluation (RTDE algorithm): if unsteady particle tracking is required (either for RANS or URANS and LES), the deposit properties like thickness, temperature, viscosity, composition and thermal resistance (fouling factor) are evaluated during the particle tracking calculation and updated in real time to predict the changes that may occur over the deposit surface. Deposit roughness is also calculated from these properties at each node.
The joint use of steady/unsteady particle tracking combined with the reduction of the computational domain allows to reduce the computational cost of the total simulation and to improve the accuracy only in the selected volume (reduced computational domain). The idea behind this approach is to reduce the number of particles that would be required for a reliable statistic analysis if either Steady or Unsteady Particle Tracking (SPT and USP) were used independently.
The first step is to perform a SPT with a sufficient number of particles over the entire domain. Deposit and trajectories statistics of this first step are calculated and used as the input of the UPT in the reduced computational domain, which represents locations researchers are most interested in where a more detailed calculation is required. A Gaussian distribution is set for each of the particle properties for each group of particles. Clusters of particle can be set within the same group, according to the given Gaussian distribution which is different for each group of particles according to the available experimental information. In this way the total number of particles to be tracked is reduced. Every particle represents a percentage of the total real mass injected according to the probability given by the Gaussian distribution for each cluster of particle.

MODELLING OF THE ENERGY RESTITUTION COEFFICIENTS

Drag, gravity and thermophoresis forces are time integrated using a Runge-Kutta 4^{th} order predictor-corrector scheme. No turbulent eddy diffusion is included. Heat exchange between particles and the surrounding environment is enabled. Thermophoresis is calculated as in He and Ahmadi (1998).
Whether a particle rebounds or sticks at the wall mainly depends on two factors: particle properties (temperature, composition, angle of impaction and kinetic energy) and impacted surface properties such as surface roughness, temperature and composition of the existing deposit layer (Walsh et al. 1990). In order to evaluate the sticking propensity of a particle, the sticking probability η_S is assumed as the key parameter. η_S can be considered as an index of the adhesion efficiency of the particle hitting on the surface. The sticking probability depends on particle and deposit properties. The sticking probability of impacting particles is usually evaluated as a function of its particle viscosity only, whereas in fact, a more rigorous approach would combine factors such as the temperature, the particle-wall viscous-elastic properties, the angle of impaction, the kinetic energy, as well as the surface roughness and stickiness (Israel and Rosner 1983, Baxter and De Sollar 1993, Huang et al. 1996) . A more detailed different approach is to calculate the energy restitution coefficient as a function of the elasticity and the plastic deformation of the particle (Stronge 2000, Quesnel 2001). This model requires the calculation of the work of adhesion/deformation of solid particles (Mittal, 2002) which is a function of the stress distribution on the particle while the particle during the impact (coupled problem): this non-linear approach is rather complicated and elastic and dump parameters are usually not known and assumed constant. Works performed during the past decade have not applied this approach to ash deposition problems yet. Deposit and adhesion of solid particles are a matter of mechanical impaction analysis as in Stronge (2000) and Thornton (1991 and 998). For temperature dependent properties, as in combustion cases, the impaction, adhesion and hence deposition process can be addressed by resorting to the theory for viscous-elastic solids behavior or better known as, namely, rheological solids (Malkin, 1994). A simplified approach can be adopted by means of the calculation of the critical velocity. This approach requires information on the particle surface (or interface) energy which depends both on the particle composition and temperature.
A simplified model for the calculation of the restitution coefficients has been used here under the following assumptions:
1. a fully plastic deformation of the particle (no elastic restitution is released from the deformed part of the particle)
2. the Young modulus E of the particle, the Poisson coefficient and the surface energy are assumed to be a function of the particle viscosity, the composition and the glass transition temperature of the particle (melting temperature)
3. normal and tangential restitution coefficient are calculated independently (decoupled problem). This simplified model is based on the studies of Thornton et al. (1991 and 1998).
The particle energy balance equation before/after the impact is:

$$\frac{1}{2}m_p\left(V_{tg}{}^2+V_n{}^2\right)_i=\frac{1}{2}m_p\left(V_{tg}{}^2+V_n{}^2\right)_f+W_{ad/d} \quad (1)$$

where $W_{ad/d}$ is the work of adhesion/deformation on the particle: since no elastic restitution in the deformed part of the particle is considered (no load/unload hysteresis cycle is considered), particles are considered fully plastic. Hence, the energy restitution coefficients are (Thornton et al., 1991 and 1998):

$$e_n = \sqrt{\left(1 - \frac{V_f^2}{V_i^2}\right)_n} \tag{2}$$

$$e_{tg} = \sqrt{\left(1 - \frac{V_f^2}{V_i^2}\right)_{tg}} \tag{3}$$

$$V_S = 1.84 \cdot \left(\frac{\frac{\Gamma^*}{r_p}}{\rho_p^3 \cdot E^{*2}} \right)^{\frac{1}{6}} \tag{4}$$

$$e_n = \sqrt{\left(1 - \frac{V_S^2}{V_i^2}\right)_n} \tag{5}$$

Where E^* and Γ^* are the equivalent Young modulus and interface energy of the wall-particle system, defined in Thornton et al., 1991 and 1998, as:

$$E^* = \frac{E_W \cdot E_p}{E_W + E_p} \tag{6}$$

$$\Gamma^* = \frac{\Gamma_W \cdot \Gamma_p}{\Gamma_W + \Gamma_p} \tag{7}$$

While to calculate e_{tg} it is required to estimate the friction between the particle and the impaction wall, the authors assumed:

$$\tau = \tau_0 \cdot \exp\left(\frac{\Gamma^*}{\mu^* + V_{tg}} \right) \tag{8}$$

$$e_{tg} = \sqrt{(1 - \tau)} \tag{9}$$

$$tg\vartheta = \frac{F_n}{F_{tg}} \tag{10}$$

where μ^* is the equivalent viscosity in $Pa \cdot s$, Γ^* is in $N \cdot m$ and τ_0 is the dynamic friction coefficient at room temperature ($300K$).

$$E = E_0 \frac{\mu}{\mu_0} \tag{11}$$

$$\Gamma = \Gamma_0 \cdot \left(\frac{\mu}{\mu_0} \right)^{1.15} \tag{12}$$

μ_0 is the viscosity at room temperature which depends upon the composition of the particle/wall surface (after deposition).

If the particle approaches the wall at a velocity lower than the sticky velocity V_S, the normal restitution coefficient is set to zero while if $tg\vartheta < \tau$, e_{tg} is then set to zero.

NUMERICAL RESULTS

Numerical results obtained using the P^3 particle diffusion model have been compared to using experimental data collected by Snyder and Lumley (1971) (see Fig. 3).

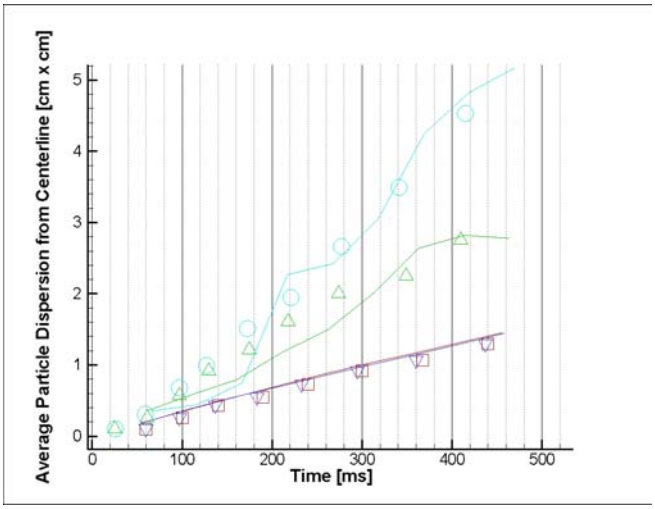

Fig. 3 Snyder and Lumley particle dispersion validation. Four cases: □ copper, ∇ solid glass, Δ hollow glass, o corn pollen. – numerical results.

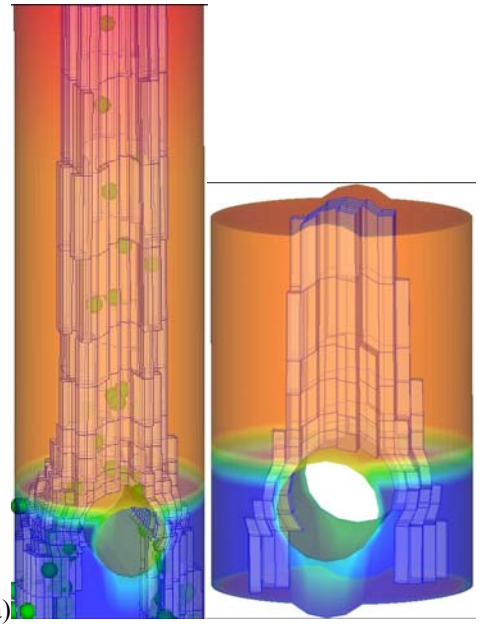

(a) (b)

Fig. 4 LCS facility. a) complete combustor with particles, b) reduced computational domain only.

RANS and LES simulations have been performed of the Lab-scale Combustion Simulator (LCS facility, see Fig. 4): RANS simulation were performed in the entire combustor while LES was calculated only in the reduced domain.
Present results can be compared with works described in Tomeczek et al. (2004). Deposition and hence adhesion of particle is calculated to yield accurate results in a fine resolution layout: RANS and LES investigations provide a more detailed information that enables researchers to optimize combustion and cleaning process. The efficiency and the accuracy of the combined use of RANS and LES has been tested on the ECN test rig for biomass combustion and ash deposition. In the ECN Lab-scale Combustor Simulator (LCS) a sampling probe is placed close to the outlet of the burner to collect part of the fouling and analyzes the thermal resistance (fouling factor) of the deposit. The probe is currently installed within the ECN Lab-scale Combustion Simulator, which is used to investigate the behavior of solid fuels under conditions which are typical for pulverized fuel fired furnaces. A full description of the LCS can be found elsewhere (Korbee et al, 2003). The probe mimics a steam pipe of a typical superheater in the early part of the convective section of a pulverized coal-fired furnace. The gas approach temperature of the probe is around 1200 °C, whereas the surface of the probe which is facing the particle-laden gas flow is controlled by the air cooling system at 500 °C.
The corresponding numerical results are quite in agreement with the experimentals. Glass particle of different size have been used to mimic deposition occurring in case of very high silicate component percentage of the ash.
In this work, numerical and experimental results on glass particles are compared to validate the deposition model (interface energy and Young Modulus as function of particle/surface viscosity hence temperature and composition of both particle and deposit) . Results are summarized in Table 1, Table 2 and Table 3.

Case	Particle Diameter	Overall LCS Temperature
Test 1	71 μm	915 °C
Test 2	105 μm	925 °C
Test 3	71 μm	1015 °C
Test 4	105 μm	1015 °C

Table 1 Experimental settings. Experimental and numerical data. Numerical simulations details: CINAR CFD code, RANS, Steady Particle Tracking, no RTDE.

Case	Experimental deposited mass	Numerical deposited mass
Test 1	0.02 g	0.511 g
Test 2	0.02 g	0.425 g
Test 3	2.07 g	1.9759 g
Test 4	1.89 g	2.8319 g

Table 2 Experimental and numerical deposited mass results. Numerical simulations details: CINAR CFD code, RANS, Steady Particle Tracking, no RTDE.

Case	Experimental deposit thickness	Numerical deposit thickness
Test 1	0.0 mm	0.3÷0.4 mm
Test 2	0.0 mm	0.1÷0.2 mm
Test 3	1.85 mm	1.9 mm
Test 4	2.8 mm	2.6 mm

Table 3 Experimental and numerical maximum deposit thickness. Numerical simulations details: CINAR CFD code, RANS, Steady Particle Tracking, no RTDE.

The agreement between numerical and experimental results is quite good for the cases test 3 and test 4 (highest oven temperature): in these cases, differences are as low as 5%. On the contrary, for test 1 and test 2, the dispersion and the deposition model over predicts the deposited mass and hence the thickness. For this reason the formulation of the Young modulus and the viscosity as function of the deposit composition and temperature appear to be not sufficient to

predict deposit thickness when deposition is most likely not to occur. Results obtained so far are considered very promising and expected to be sufficiently accurate to predict the deposit in a wider range of cases such as slurry, water scale deposition and fouling along pipelines in the next future.

As shown in a few FLUENT LES simulation snapshots in Fig. 6 and Fig. 7 deposit growth is locally predicted.

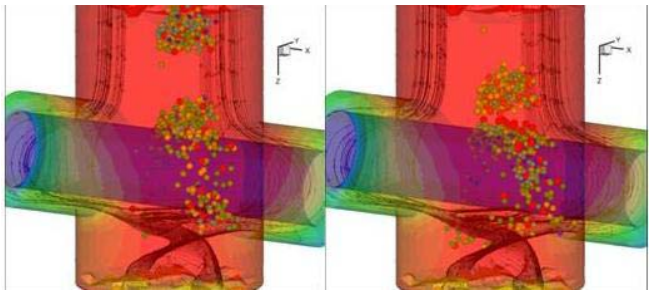

Fig. 5 Unsteady particle tracking in FLUENT LES CFD simulation. Instant Snapshot. It is highlighted the influence of the turbulence in the particle motion-dispersion in the LCS facility. The turbulence and the vortex generated by the probe are highlighted.

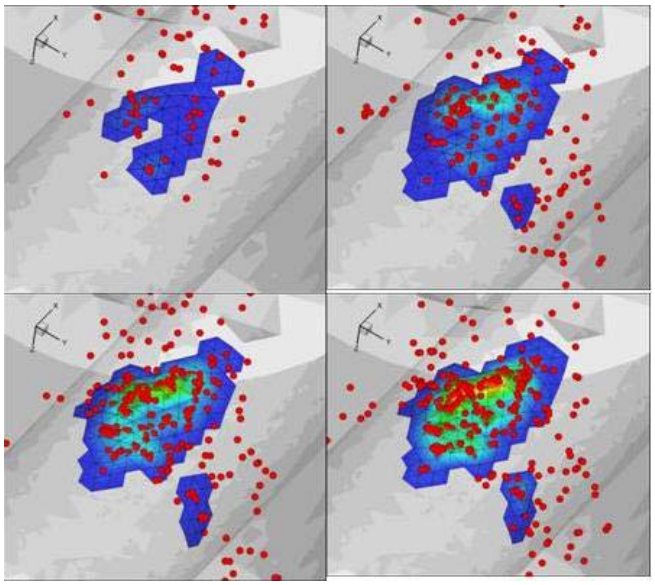

Fig 6 Glass particle deposit growth in FLUENT LES simulation. Particle deposition and deposit growth at 0.1 s, 0.2 s, 0.3 s and 0.4 s.

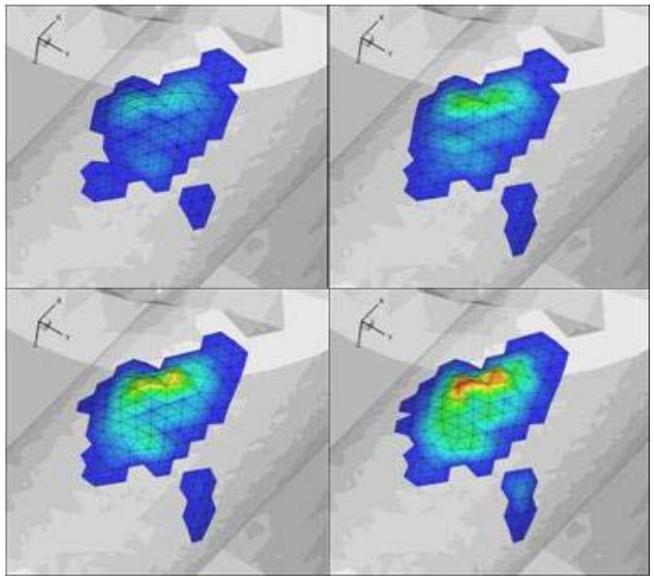

Fig 7 Deposit growth at 0.1 s, 0.2 s, 0.3 s and 0.4 s. Real time deposit evaluation enabled. These picture are taken from the same simulation showed in Fig. 6.

CONCLUSIONS

A novel computer code that elaborates particle trajectories by post-processing CFD data has been presented. This code has been developed to provide both a numerical estimate of ash deposition in pulverized coal/biomass burners predict of loss performance in heat exchange. Experimental results collected from the LCS facility have been used to validate numerical results. The presented code elaborates hybrid unstructured P1 element meshes. A specific 2 step tracking particles algorithm has been implemented. The main features of the code are concerning both computational strategy implemented into the P^3 and the modeling of the deposition process that links impact mechanics of "cold" elastic particles and adhesion of "hot" plastic particles. These topics are summarized as it follows:

1. The 2 step particle detection in conjunction with the trilinear-isoparametrical interpolation enables the P^3 code to be CPU time almost mesh independent and to perform particle deposition with real time deposit growth despite the distortion of the mesh that may occur due to the deposit growth.
2. The P^3 code is based on multi-CFD capability. The code is capable of elaborate 3D unstructured hybrid meshes from FLUENT, CINAR and CFX.
3. The P^3 computes steady/unsteady particle tracking on RANS/URANS and LES CFD simulation.

4. Particle dispersion modeling is based on the κ-ε model (Random Walk Approach) and is validated on Snyder and Lumley data.
5. For FLUENT only, it is possible to export the deposited mesh, (namely a new mesh whose shape has been modified to include the deposit), to perform a CFD calculation on the fluid (gas or liquid) phase.
6. The deposition model is based on the evaluation of the critical velocity. An ad hoc formulation for high silicate/ glass particles concerning the Young modulus, the Poisson coefficient and the particle-wall surface energy has been presented.

The selected benchmark cases demonstrated the potentials of the code as well as some inaccuracies in the deposit prediction. Results obtained so far are substantially in agreement with the experimentals and encourage the authors to further pursue such multi-CFD particle post-processing approach and investigate new possible applications.

NOMENCLATURE

e restitution coefficient (nondimensional)

m mass, kg

r particle radius, m

E Young modulus, Pa

V Velocity, m/s

W Work adhesion/deformation, J

Γ surface energy, N/m

ϑ friction angle, rad

μ viscosity, $Pa \cdot s$

τ friction coefficient (nondimensional)

Sub/Superscript

ad adhesion

i impact

f final

n normal direction (normal to wall)

p particle

w wall

S sticky

tg tangential direction (tangential to wall)

0 parameter calculated at room temperature

$*$ equivalent parameter.

REFERENCES

L.L. Baxter, R.E. Mitchell, 1992, Release of Iron During the Combustion of Illinois No. 6 Coal. Combust. Flame, Vol. 88, Pag. 1-14.

L.L. Baxter, R.W. De Sollar, 1993, A mechanistic description of ash deposition during pulverized coal combustion: predictions compared with observations, Fuel Vol 72, Issue 10, Pag. 1411-1418.

C. He, G. Ahmadi, Particle, 1998, Deposition with thermophoresis in laminar and turbulent duct flows, Aerosol Science and Technology, Vol. 29, Issue 6, pag. 525-546.

L. Y. Huang, J. S. Norman, M. Pourkashanian and A. Williams, 1996, Prediction of ash deposition on superheater tubes from pulverized coal combustion, Fuel, Vol. 75, Issue 3, pp 271-279.

R. Israel, D. E. Rosner, 1983, Use of a generalized stokes number to determine the aerodynamic capture efficiency of non-stokesian particles for a compressible gas flow. Aerosol Sci. & Tech. 2, Pag. 45–51.

R. Korbee,A.R. Boersma, M.K. Cieplik, P.G.Th. Heere, D.J. Slort, J.H.A. Kiel, 2003, Fuel characterisation and test methods for biomass co-firing, Report ECN-C-03-057, p.41.

A.Y. Malkin, 1994, *Rheology Fundamentals*, Canada ChemTec Publishing.

K.L. Mittal, 2002, *Contact angle, wettability and adhesion*. Vol.2, Utrecht VSP.

D.J. Quesnel, D.S. Rimai, L.H. Sharpe, 2001, *Particle adhesion: application and advances*, New York Taylor and Francis.

W,H. Snyder and L. Lumley. 1971, Some measurements of particle velocity autocorrelation functions in turbulent flow, J.Fluid Mech.,vol 48, part 1, pp. 41-71.

Senior, C. and Srinivasachar, S. (1995) "Viscosity of ash particles in combustion systems for prediction of particle sticking." Energy and Fuels, 9, pp. 277–283.

S. Srinivasachar, J.J. Helble, A.A. Boni, 1990, Mineral behavior during coal combustion 1. Pyrite transformations, Progr. Energy Combust. Sci., 16, Pag. 281-292.

S. Srinivasachar S., J.J. Helble, A.A. Boni, N. Shah, G.P. Huffman and F.E. Huggins, 1990, Mineral behavior during coal combustion 2. Illite transformations, Progr. Energy Combust. Sci. Vol. 16, Pag. 293-302.

W.J. Stronge, 2000, *Impact Mechanics*, Cambridge University Press.

C. Thornton, K.K. Yin, 1991, Impact of elastic spheres with and without adhesion, Powder Technology, vol 65, pag. 153-166.

C. Thornton, Z. Ning, 1998, A theoretical model for the stick/bounce behaviour of adhesive elastic-plastic spheres, Powder Technology, vol 99, pag. 154-162.

J. Tomeczek, H. Palugniok, J. Ochman, 2004, Modelling of deposit formation on heating tubes in pulverized coal boilers, Fuel Vol 83, pp. 213-221.

P.M. Walsh, A.N. Sayre, D.O. Loehden, L.S. Monroe, J.M. Beer, A.F. Sarofim, 1990, Progr. Energy Combust. Sci., 16, 327.